BioResearch Open Access
Volume 2, Number 4, August 2013

DOI: 10.1089/biores.2013.0016

A Comparative Analysis of the *In Vitro* Effects of Pulsed Electromagnetic Field Treatment on Osteogenic Differentiation of Two Different Mesenchymal Cell Lineages

Gabriele Ceccarelli,[1,2,*] Nora Bloise,[2,3,*] Melissa Mantelli,[4] Giulia Gastaldi,[2,3] Lorenzo Fassina,[2,5] Maria Gabriella Cusella De Angelis,[1,2] Davide Ferrari,[6] Marcello Imbriani,[1,7] and Livia Visai[2,3,7]

Abstract

Human mesenchymal stem cells (MSCs) are a promising candidate cell type for regenerative medicine and tissue engineering applications. Exposure of MSCs to physical stimuli favors early and rapid activation of the tissue repair process. In this study we investigated the *in vitro* effects of pulsed electromagnetic field (PEMF) treatment on the proliferation and osteogenic differentiation of bone marrow MSCs (BM-MSCs) and adipose-tissue MSCs (ASCs), to assess if both types of MSCs could be indifferently used in combination with PEMF exposure for bone tissue healing. We compared the cell viability, cell matrix distribution, and calcified matrix production in unstimulated and PEMF-stimulated (magnetic field: 2 mT, amplitude: 5 mV) mesenchymal cell lineages. After PEMF exposure, in comparison with ASCs, BM-MSCs showed an increase in cell proliferation ($p < 0.05$) and an enhanced deposition of extracellular matrix components such as decorin, fibronectin, osteocalcin, osteonectin, osteopontin, and type-I and -III collagens ($p < 0.05$). Calcium deposition was 1.5-fold greater in BM-MSC–derived osteoblasts ($p < 0.05$). The immunofluorescence related to the deposition of bone matrix proteins and calcium showed their colocalization to the cell-rich areas for both types of MSC-derived osteoblast. Alkaline phosphatase activity increased nearly 2-fold ($p < 0.001$) and its protein content was 1.2-fold higher in osteoblasts derived from BM-MSCs. The quantitative reverse-transcription polymerase chain reaction (qRT-PCR) analysis revealed up-regulated transcription specific for bone sialoprotein, osteopontin, osteonectin, and Runx2, but at a higher level for cells differentiated from BM-MSCs. All together these results suggest that PEMF promotion of bone extracellular matrix deposition is more efficient in osteoblasts differentiated from BM-MSCs.

Key words: human adipose-derived stem cells; human mesenchymal stem cells; osteogenic differentiation; pulsed electromagnetic field

Introduction

The use of stem cells in regenerative medicine is an appealing area of research that has received a great deal of attention in recent years. Ideally, stem cells for regenerative medicinal applications should meet the following set of criteria: they should be (i) found in abundant quantities (millions to billions of cells); (ii) readily collected and harvested by a minimally invasive procedure; (iii) differentiated along multiple cell lineage pathways in a reproducible manner; (iv) safely and effectively transplanted to either an autologous or allogeneic host.[1,2] The use of totipotent and multipotent stem cells in regenerative medicine has opened the way for autologous tissue transplantation. However, mesenchymal stem cell (MSC) concentration in bone marrow (BM) transplants is lower with respect to cultured cells. It also has to

Departments of [1]Public Health, Neuroscience, and Experimental & Forensic Medicine [3]Molecular Medicine, and [5]Electrical, Computer, & Biomedical Engineering; [2]Center for Tissue Engineering (C.I.T.); University of Pavia, Pavia, Italy.
[4]Immunology and Transplant Laboratory, Pediatric Onco-Hematology Department, Fondazione IRCCS Policlinico S. Matteo, Pavia, Italy.
[6]Bioscience, University of Parma, Parma, Italy.
[7]Department of Occupational Medicine, Ergonomics and Disability, Laboratory of Nanotechnology, Salvatore Maugeri Foundation, IRCCS, Pavia, Italy.
*Both authors contributed equally to this article.

be considered that cell amplification by culture is not free from the dangers of bacterial contamination, xenogenic risk, or cellular transformation, influencing MSC differentiation capacities. It is still necessary to perform more clinical trials to select the best treatment modality to repair bone tissue.[3,4]

Although BM-derived MSCs (BM-MSCs) are being widely used in cell-based therapy and tissue engineering, adipose-derived MSCs (ASCs) might serve as an alternative source of MSCs. In the setting of an autologous implant, the use of ASCs as a cell source for bone therapeutic applications presents many potential advantages in comparison with BM-MSCs. Subcutaneous adipose depots are accessible, abundant, and replenishable, thereby providing a potential adult stem cell reservoir for each individual.[5–10] Aside from the use of MSCs, different types of approach have been applied in order to improve osteoinduction and consequently to reduce the differentiation period. Many biomaterials have been tested,[11–13] and following a "biomimetic" approach, different bioreactors have been used to improve osteogenesis.[14–16] Biophysical stimulation (i.e., pulsed electromagnetic fields [PEMF] or low-intensity pulsed ultrasound) has been used in clinical settings to accelerate and finalize the healing process of a fresh fracture, or a fracture at risk of nonunion, and to enhance the spontaneous repair capability of the bone tissue (i.e., to reactivate the healing process in pathological conditions such as delayed union or pseudoarthrosis).[17] In particular, PEMFs have been widely used in orthopedics for at least three decades,[18,19] but as far as we know a comparative analysis to evaluate their potential effects on *in vitro* culture of both BM-MSCs and ASCs has not been performed.

PEMF therapy is approved for bone disorders in animals and in humans, including nonunited bone fracture healing, pseudoarthrosis, and osteoporosis.[20–22] PEMF treatment reportedly aids the healing of osteotomies[23] and has been applied clinically to promote bone healing for many years.[24] Clinical effectiveness was initially thought to be due to the accelerated formation of bone matrix by the weak electric current generated by the magnetic field[25] in animal experiments,[26,27] based on studies that indicated that electromagnetic fields may heal bone fractures and slow down bone matrix loss. Current studies on stem cells have revealed that the regeneration of human body tissues and supplementation of mature functioning cells are due to the proliferation and differentiation of stem cells.[28–31] The mechanism of action underlying how PEMF promotes the formation of bone in an *in vitro* environment remains elusive. The electromagnetic stimulation raises the net Ca^{2+} flux in human osteoblast-like cells,[32] and, according to Pavalko's diffusion-controlled/solid state signaling model,[33] the increase in the cytosolic Ca^{2+} concentration is the starting point for signaling pathways targeting specific bone matrix genes. Considering the model of Pavalko, the analysis of the transcripts specific for decorin, osteopontin, and type-I collagen revealed, concordantly, that the application of the electromagnetic wave caused an increase in gene transcription. In recent published studies, it was reported that PEMF exposure could enhance early cell proliferation in BM-MSC–mediated osteogenesis and accelerate osteogenesis.[34,35]

In view of a tissue engineering approach for bone repair, the aim of this study was to assess if the application of a physical stimulus could have a biological effect on human BM-MSCs and ASCs. Therefore we investigated the influence of PEMF on the proliferation and differentiation of both types of MSCs in terms of osteoblast morphology, proliferation, and deposition of a mineralized extracellular matrix (ECM). Considering the possible clinical application of PEMF in support of skeletal therapy, the final scope of this study was to perform a comparative analysis on the efficacy of electromagnetic treatment in both types of stem cell lineage for *in vivo* bone development. To the best of our knowledge, this is the first comparative analysis on this topic.

Materials and Methods

Electromagnetic bioreactor apparatus

The electromagnetic bioreactor consisted of a supporting structure custom-designed in a tube of polymethylmethacrylate; the windowed tube had a well-plate and two solenoids (Helmoltz coils, the planes of which were parallel).[35] In this experimental setup, the magnetic field and the induced electric field were perpendicular and parallel to the scaffold surfaces, respectively. The cell surfaces were 5 cm away from the solenoid plane, and the solenoids were powered by a Biostim SPT pulse generator (Igea, Carpi, Italy), which generated PEMFs. Given the position of the solenoids and the characteristics of the pulse generator, the electromagnetic stimulation had the following parameters: magnetic field intensity equal to 2 ± 0.2 mT, induced electric tension amplitude equal to 5 ± 1 mV, signal frequency of 75 ± 2 Hz, and pulse duration of ~ 1.3 msec.[36] The magnetic field was measured with a Hall Effect transverse gaussmeter probe (Sypris Solutions, Louisville, KY) and gaussmeter (Laboratorio Elettrofisico, Milan, Italy), the induced electric tension was measured with a standard coil probe, and the temporal pattern of the electromagnetic signal was evaluated by a digital oscilloscope (LeCroy, Chestnut Ridge, NY). In clinical settings the PEMF parameters were similar, but a period of 30–40 min represented the exposure time for tissues or organs. As shown in this *in vitro* study, the PEMF biological effect was directly evaluated on both stem cells and the exposure time was determined experimentally. In our experimental settings, the electromagnetic bioreactor was placed into a standard cell culture incubator in a 37°C, 5% CO_2 environment.

Isolation, expansion, and culture of BM-MSCs and ASCs

The design of this study was approved by the Institutional Review Board of the Fondazione IRCCS Policlinico San Matteo and the University of Pavia (2011).

BM-MSCs. BM aspirates were harvested from healthy pediatric hematopoietic stem cell donors after obtaining written informed consent. Thirty milliliters of BM from each donor was assigned to BM-MSC generation; heparin was added as an anticoagulant. Mononuclear cells were isolated from BM aspirates (30 mL) by Ficoll density gradient centrifugation (density, 1.077 g/mL; Lymphoprep, Nycomed Pharma, Oslo, Norway) and plated in noncoated 75- to 175-cm^2 polystyrene culture flasks (Corning Costar, Celbio, Milan, Italy) at a density of 16×10^4 cells/cm^2. Cells were cultured in Mesencult medium (Stem Cell Technologies, Vancouver, Canada) supplemented with 2 mM L-glutamine, 50 μg/mL gentamycin, and 10% fetal calf serum. Cultures were maintained at 37°C in a humidified atmosphere containing 5% CO_2. After 48 h, nonadherent cells were discarded and culture medium was replaced twice a week. After reaching 80%

confluence as a minimum, the cells were harvested and replated for expansion at a density of 4000 cells/cm^2 until the fifth passage. The colony-forming unit fibroblast assay (CFU-F) was performed as described previously.[37] CFU-F formation was examined after 12 days of incubation in a humidified atmosphere (37°C, 5% CO_2); the clonogenic efficiency was calculated as the number of colonies per 10^6 BM mononuclear cells seeded. According to the International Society for Cellular Therapy on the nomenclature of mesenchymal progenitors, the cells cultured for this study were defined as multipotent stromal cells. To phenotypically characterize BM-MSCs and to define their purity, FACS analysis was performed as previously described.[37] After reaching 80% confluence at a minimum, the cells were harvested and replated for expansion at a density of 2.5×10^4 cells/cm^2. The cells were cultured at 37°C, 5% CO_2, and three fifths of the medium was renewed every 3 days.

Adipose-tissue MSCs. Subcutaneous adipose tissue was obtained from healthy pediatric donors during orthopedic surgery. Informed consent was obtained before the surgical intervention. In brief, the tissue was finely minced and then incubated in digestion buffer (0.01% collagenase type-II in Dulbecco's modified Eagle's medium [DMEM] F12-HAM medium supplemented with 10% fetal calf serum, 100 U penicillin/streptomycin, amphotericin) for 1 h at 37°C with vigorously shaking. At the end of the incubation, five volumes of DMEM F12-HAM were added to neutralize the collagenase, and the suspension was centrifuged at 800 g for 10 min. The resulting pellet, containing ASCs, was suspended in DMEM F12-HAM supplemented with 10% fetal bovine serum, and 100 UI penicillin/streptomycin and amphotericin (control medium, CM). The ASCs were initially cultured in CM up to 95% confluence in a humidified atmosphere, 95% air with 5% CO_2 at 37°C. The adherent cells were trypsinized and 1×10^5 ASCs per 100-mm^2 tissue culture plate were seeded in flasks. These passages were repeated three times. To phenotypically characterize ASCs and to define their purity, FACS analysis was performed as described.[38]

Cell culture conditions: unstimulated and PEMF stimulated

A suspension (5×10^5) of both types of stem cell in 200 μL of proliferative medium (PM) was seeded in 24-well tissue culture plates and allowed to attach overnight. Then, the medium was replaced with osteogenic medium (OM) and changed every 3 days: α-MEM (Invitrogen, Paisley, PENN) supplemented with 10% fetal bovine serum, 50 μg/mL penicillin-streptomycin, 1% L-glutamine, 10^{-7} dexamethasone, 50 μg/mL ascorbic acid, and 5 mM β-glycerophosphate.[39]

The "electromagnetic culture" was stimulated with PEMF for 5, 10, and 30 min and 1, 4, and 8 h per day for 7 days in PM, whereas the "static culture" or non–PEMF-stimulated culture was incubated for the same amount of time in PM in standard well-plates culture placed in a CO_2 incubator far from the electromagnetic bioreactor.

The osteogenic differentiation of both types of stem cell lineages was performed for 21 days with or without PEMF exposure in OM.

3-(4,5-dimethylthiazole-2-yl)-2,5-diphenyl tetrazolium bromide test

To evaluate the mitochondrial activity of both cultured cell conditions, a test with 3-(4,5-dimethylthiazole-2-yl)-2,5-diphenyl tetrazolium bromide (MTT; Sigma-Aldrich, St. Louis, MO), was performed on day 7 in PM as previously reported[40] on the unstimulated and PEMF-stimulated cultures at different exposure times. The viability assay was also performed on days 7, 14, and 21 (end of the culture period) on the unstimulated and PEMF-stimulated cultures of both cell types. Aliquots of 200 μL were sampled, and the related absorbance values were measured at 570 nm by a microplate reader (BioRad Laboratories, Hercules, CA). A standard cell viability curve was used and the results were expressed as percentage referred to both type of unstimulated cells, respectively.

Apoptosis

Apoptosis is defined as programmed, physiological cell death and plays an important role in tissue homeostasis. The Annexin V technique detects apoptosis by targeting the loss of phospholipid asymmetry in the plasma membrane. The loss of plasma membrane asymmetry is an early event in apoptosis, independent of cell type, resulting in the exposure of phosphatidylserine (PS) residues at the outer plasma membrane leaflet.[41]

The Annexin V-FITC Apoptosis Detection Kit (Bender Medsystems, Vienna, Austria) was used according to the manufacturer's instructions.

DNA content

At the end of incubation, the cells were lysed by a freeze–thaw method in sterile deionized distilled water. The released DNA content was evaluated with a fluorometric DNA quantification kit (PicoGreen; Molecular Probes, Eugene, OR). A DNA standard curve[40] obtained from a known amount of osteoblasts was used to express the results as cell numbers per well.

Confocal laser scanning microscopy analysis

The cells were fixed with 4% (w/v) paraformaldehyde solution in 0.1 M phosphate buffer (pH 7.4) for 8 h at room temperature and washed with phosphate-buffered saline (PBS) three times for 15 min. Then, the unstimulated and PEMF stimulated cells were treated as described in the following sections.

Adhesion and morphological analysis. For adhesion and morphological analysis, paraformaldehyde fixed cells were permeabilized with 0.1% Triton X-100 for 1 h at room temperature (RT) and incubated with phalloidin (Alexa-Fluor-488 phalloidin, Invitrogen) for 20 min. Then the cells were further incubated overnight at 4°C with the primary and antivinculin clone (hVIN-1, Sigma-Aldrich). Finally, after staining with Alexa-Fluor-633–conjugated secondary antibodies (Invitrogen) for 1 h at RT, samples were mounted and nuclei were counterstained with Hoechst (Sigma Aldrich).

Immunological studies. For immunological studies, paraformaldehyde fixed cells were blocked by incubating with PAT (PBS containing 1% [w/v] bovine serum albumin and 0.02% [v/v] Tween 20) for 2 h at room temperature and washed. Anti–type-I and -III collagens, antidecorin, anti-osteopontin, anti-osteocalcin, anti-osteonectin, and anti–alkaline phosphatase (anti-ALP) rabbit polyclonal antisera were used as the primary antibodies diluted to 1:500 in

PAT. The same dilution was used with anti-fibronectin (anti-FN) rabbit polyclonal IgG. The incubation with the primary antibodies was performed overnight at 4°C, whereas the negative controls were incubated with PAT alone. The samples and the negative controls were washed and incubated with Alexa-Fluor-488 goat antirabbit IgG (HþL; Invitrogen) at a dilution of 1:750 in PAT for 1 h at room temperature. At the end of the incubation, the samples were washed in PBS, counterstained with a Hoechst solution (2 μg/mL) to target the cellular nuclei, and then washed.

The images were taken by the TCS SPII confocal microscope (Leica Microsystems, Bensheim, Germany) equipped with a digital image capture system at 40× magnification.

Scanning electron microscopy analysis

Both types of cell were also seeded on plastic cell culture coverslip disks (Thermanox Plastic, Nalge Nunc International, New York, NY) and cultured as previously indicated. After 3 weeks of culture, cells were fixed with 2.5% (v/v) glutaraldehyde solution in 0.1 M sodium cacodylate buffer (pH = 7.2) for 1 h at 4°C, washed with sodium cacodylate buffer, and then dehydrated at room temperature in an ethanol gradient series up to 100%. The samples were kept in 100% ethanol for 15 min, and then critical-point dried with CO_2. The specimens were spatter-coated with gold and observed at 50× and 1000× magnification respectively with a Leica Cambridge Stereoscan 440 microscope (Leica Microsystems, Bensheim, Germany) at 8 kV.[42]

Gene expression analyses

Total RNA from the stimulated samples (treat) and the nonstimulated samples (control) was extracted with the Trizol reagent (Invitrogen) and retrotranscribed into cDNA with the iScript cDNA Synthesis Kit (BioRad Laboratories) as previously reported.[42]

Quantitative reverse-transcription polymerase chain reaction (qRT-PCR) analysis was performed in a 48-well optical reaction plate using a MiniOpticon Real-Time PCR System (BioRad Laboratories). Oligonucleotide primers were designed with gene sequences published in GenBank and are indicated in Table 1. Reactions were performed in 20 mL with 2 mL of cDNA, 10 mL Brilliant SYBER Green qPCR Master Mix (Stratagene, La Jolla, CA), 0.4 mL of each primer, and 7.2 mL H_2O. PCR conditions were as follows: 3 min at 95°C, 30 cycles of 5 sec at 95°C, and 23 sec at 60°C. Gene expression was normalized to the GAPDH housekeeping gene expression. Each sample was analyzed in triplicate and correlated against a standard curve. The reaction mixture, without cDNA, was used as a negative control in each run.

Purified proteins

Decorin, type-I collagen, and fibronectin were purified as described previously[42]; osteocalcin was acquired from Biomedical Technologies, Inc. (Stoughton, MA), osteopontin and osteonectin were obtained from Assay Designs, Inc. (Ann Arbor, MI); and type-III collagen and ALP were purchased from Sigma-Aldrich, Inc.

Polyclonal antisera

Dr. Larry W. Fisher (http://csdb.nidcr.nih.gov/csdb/antisera.htm, National Institutes of Health, Bethesda, MD) provided us with the rabbit polyclonal anti–type-I and -III collagen, antidecorin, anti-osteopontin, anti-osteocalcin, anti-osteonectin, and anti-ALP. Polyclonal antibody against human fibronectin was produced as previously described.[40]

Extraction of ECM proteins from the cultured scaffolds and enzyme-linked immunosorbent assay

At the end of the culture period, in order to evaluate the amount of ECM produced, the samples were washed extensively with sterile PBS to remove culture medium, and then incubated for 24 h at 37°C with 1 mL of sterile sample buffer (20 mM Tris-HCl, 4 M GuHCl, 10 mM EDTA, 0.066% [w/v] sodium dodecyl sulfate [SDS], pH 8.0). At the end of the incubation period, the total protein concentration in both culture systems was evaluated with the BCA Protein Assay Kit (Pierce Biotechnology, Inc., Rockford, IL). The total protein concentration was 90.1 ± 7.1 μg/mL for the unstimulated BM-MSCs and 118.5 ± 8.2 μg/mL for the PEMF–stimulated BM-MSCs, 85.7 ± 2.5 μg/mL for the unstimulated ASCs and 105.0 ± 3.3 μg/mL for the PEMF-stimulated ASCs.

Calibration curves to measure type-I and -III collagens, decorin, osteopontin, osteocalcin, osteonectin, fibronectin, and APT were performed as previously described.[39] In order to measure the ECM amount of each protein an enzyme-linked immunosorbent assay (ELISA) was performed as previously reported.[42]

We have taken into consideration that an underestimation of the absolute protein deposition is possible because the sample buffer, used for matrix extraction, contains SDS, which may interfere with protein adsorption during the ELISA. The amount of ECM constituents from both samples was expressed as pg/(cells per well).

Quantification of calcium

To evaluate the calcium deposition, fluorescent calcein detection and calcium–cresolphthalein complexone methods were performed as described previously.[42]

Calcein. At the end of cell incubation, each sample was rinsed with sterile PBS and stained with a calcein solution

Table 1. Primers Used for Quantitative Reverse-Transcription Polymerase Chain Reaction

Gene	*Upstream primer*	*Downstream primer*
BOSP	5′-GGG CAG TAG TGA CTC ATC CG-3′	5′-TCA GCC TCA GAG TCT TCA TCT TC-3′
GAPDH	5′-AGC CTC AAG ATC ATC AGC AAT GCC-3′	5′-TGT GGT CAT GAG TCC TTC CAC GAT-3′
OP	5′-GTG ATT TGC TTT TGC CTC CT-3′	5′-GCC ACA GCA TCT GGG TAT TT-3′
RUNX2	5′-ACA GTA GAT GGA CCT CGG GA-3′	5′-ATA CTG GGA TGA GGA ATG CG-3′
OSN	5′-CTT CAG ACT GCC CGG AGA-3′	5′-GAA AGA AGA TCC AGG CCC TC-3′

(5 mM in PBS; Invitrogen, Carlsbad, CA) for 30 min at 22°C. The samples were counterstained with a Hoechst solution (2 μg/mL) to target the cellular nuclei, and then washed with PBS. The images were taken by the TCS SPII confocal microscope (Leica Microsystems) equipped with a digital image capture system at 40× magnification.

Calcium–cresolphthalein complexone method. In order to evaluate calcium deposition, the calcium–cresolphthalein complexone method was performed as previously described[43] on cells cultured with or without PEMF. Briefly, the calcium content of each sample was assayed to quantify the amount of mineralized matrix present, using a Calcium Fast kit (Mercury SPA, Naples, Italy) according to the manufacturer's instructions as previously described.[42] Samples were run in triplicate and compared with the calibration curve of standards.

ALP activity

ALP activity was determined using a colorimetric end point assay.[40] The assay measures the conversion of the colorless substrate *p*-nitrophenol phosphate (PNPP) by the enzyme ALP to the yellow product *p*-nitrophenol; the rate of color change corresponds with the amount of enzyme present in solution. The test was performed as previously described[42] on cells cultured with or without PEMF stimulation. Samples were run in triplicate and compared with the calibration curve of *p*-nitrophenol standards. The enzyme activity was expressed as micromoles of *p*-nitrophenol produced per minute per milligram of enzyme.

Statistics

Each experiment was repeated three times. Results are expressed as the mean ± standard deviation. In order to compare the results between the two types of sample unstimulated or PEMF-stimulated, the one-way analysis of variance (ANOVA) with *post hoc* Bonferroni test was applied, with a significance level of 0.05.

Results

The isolated, expanded, and characterized human stem cells harvested from BM aspirates or obtained surgically from subcutaneous adipose tissue of pediatric donors were seeded onto 24-well culture plates and then cultivated in proliferative culture conditions in the absence (control) or presence of an electromagnetic bioreactor for 7 days (Fig. 1). To determine the best exposure time for PEMF stimulation, an MTT test was performed at day 7 on both stem cell cultures stimulated for 5, 10, and 30 min and 1, 4, and 8 h per day. The results were compared to the unstimulated cells set at 100% cell viability. We found that 10 min of PEMF stimulation was the optimal culture condition for both cell types (Fig. 1). At higher PEMF doses, cell viability of both stem cells was lower compared to the controls.

To assess if both types of stem cells could be indifferently used in combination with PEMF exposure to improve bone tissue repair, BM-MSCs and ASCs were cultivated in the absence or presence of an electromagnetic bioreactor for 21 days. To evaluate the effect simply due to PEMF exposition, both stem cells were cultivated in OM since ASCs in osteogenic culture conditions are observed to express genes and proteins associated with the osteoblast phenotype. As indicated in Figure 1, the two MSCs lineages were exposed to PEMF for 10 min per day and compared to unstimulated cells. This culture system allowed the study of both stem cell types as they proliferated and differentiated to osteoblasts producing a calcified ECM in an inactive or electromagnetically active environment. We compared the cell viability, cell matrix distribution, and calcified matrix production of the unstimulated and PEMF-stimulated culture systems for both types of mesenchymal cell lineages.

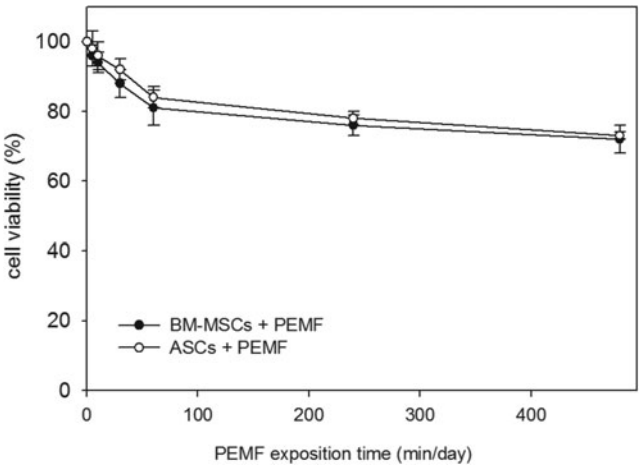

FIG. 1. Effect of pulsed electromagnetic field (PEMF) exposure on bone marrow mesenchymal stem cell (BM-MSC) and adipose tissue mesenchymal stem cells (ASC) viability. A cell viability assay was performed at day 7 of culture stimulating both types of stem cells for 5, 10, and 30 min and 1, 4, and 8 h/day with a PEMF in proliferative medium. The controls were represented by unstimulated BM-MSCs and ASCs and were set as 100% cell viability. The data were represented as a percentage of the control. Bars indicate mean values ± standard error of the mean of results from three experiments.

Cell viability and morphology

On days 7 and 14 and at the end of the culture (on day 21), the average cell viability for the unstimulated or PEMF stimulated was in the 88%–95% range with no statistically significant differences between cell types, unstimulated or PEMF-stimulated ($p > 0.05$). The percentage of viability was as follows: on days 7, BM-MSCs + PEMF, 88% ± 6.1%; ASCs + PEMF, 90% ± 8.2 %; on day 14, BM-MSCs + PEMF, 94% ± 9%; ASCs + PEMF, 93% ± 7.5%; and on day 21, BM-MSCs + PEMF, 95% ± 9%; ASCs + PEMF, 94.4% ± 7.8%. Additional experiments were then performed.

After 21 days in comparison with unstimulated cells, greater proliferation of both cell types was observed with PEMF exposure: the measurement of the DNA content in the static culture showed an increase in cell number per well from $3.7 \times 10^4 \pm 8.2 \times 10^2$ up to $5.1 \times 10^4 \pm 8.4 \times 10^2$ ($p < 0.05$) in the dynamic culture for BM-MSC–derived cells. A similar increase was observed for ASC-derived cells: from $4.2 \times 10^5 \pm 8.2 \times 10^2$ up to $5.4 \times 10^4 \pm 8.4 \times 10^2$ ($p < 0.05$) cell number per well. Because the DNA may remain entrapped in the calcified matrix, an underestimation of culture cellularity is possible.

To determine whether PEMF treatment provoked cell apoptosis Annexin V and propidium iodide (PI) staining was performed. On the same days as the MTT test, confocal laser scanning microscopy (CLSM) analysis was performed on both unstimulated and PEMF-stimulated cells. It is known that in the early stages of apoptosis, the plasma membrane excludes viability dyes such as PI, therefore cells that display only Annexin V staining (PI negative) are in the early stages of apoptosis. During late-stage apoptosis, loss of cell membrane integrity allows Annexin V binding to cytosolic PS, as well as cell uptake of PI. In view of this, CLSM analysis of unstimulated and PEMF-stimulated BM-MSCs and ASCs were negative after Annexin V and PI staining (data not shown), indicating that the PEMF stimulation did not induce apoptosis in either type of cell.

To qualitatively evaluate cell viability and morphology, cells were also observed by CLSM (Fig. 2B) and by scanning electron microscopy (SEM; Fig. 2A) at the end of the culture period. CLSM observations revealed an equivalent cell morphology in both types of culture condition (Fig. 2B), suggesting that the PEMF stimulation did not alter cell viability or proliferation. In particular, stimulated cells (Fig. 2B-ii, iv) showed better cytoskeleton organization with F-actin–containing fibers arranged as straight, cable-like cords transversing the cytoplasm.

Figure 2A is a representative SEM image of 21 days in cell culture showing adherence and morphology of both types of cell, unstimulated and PEMF-stimulated. In particular, independently of the stem cell source, osteoblasts grown in PEMF (Fig. 2A-ii, iv) homogeneously covered the wells in comparison with unstimulated cells (Fig. 2A-i, iii). At higher magnification, no significant morphological differences for either cell type or culture condition were observed: cells were flat and compact.

Characterization of gene expression in bone

To characterize the gene expression in both types of cell and culture system condition, RT-PCR and qRT-PCR analyses were performed after 7 and 21 days of culture. On day 7, the qualitative RT-PCR and qRT-PCR did not show a significant difference in the gene expression levels for ECM proteins in either cell or culture system condition (data not shown). The main difference in gene expression levels between cell types and culture conditions was observed after 21 days of culture.

At the end of the cell culture period, the qRT-PCR performed on both cell types and culture system condition showed some differences. It revealed a bright band on the agarose gel for all indicated genes and particularly for the transcripts specific for bone sialoprotein, osteopontin, osteonectin (data not shown).

To further examine these data, a qRT-PCR for gene expression profiles of bone-specific proteins and transcriptional factor Runx2 was performed after 21 days using the $\Delta\Delta$Ct method. The results showed a significantly enhanced fold difference for bone sialoprotein (BOSP), osteopontin (OP), osteonectin (OSN), and Runt-related transcription factor 2 (Runx2) ($p < 0.001$; Fig. 3A) in PEMF-stimulated cells of BM origin in comparison with the unstimulated cells. No evident fold difference was detected for gene expression profiles of the same proteins between the unstimulated and PEMF-stimulated cells deriving from human adipose tissue ($p > 0.05$; Fig. 3B).

Characterization of calcified ECM deposition

At the end of the cell culture, immunolocalization of osteopontin and osteocalcin showed a more intense green fluorescence in osteoblasts differentiated from BM-MSC and exposed to PEMF (Fig. 4A-ii and B-ii), revealing the stimulatory effect of the physical stimulation in terms of higher cell proliferation and more intense fluorescent staining of the ECM. Unstimulated cells were few and surrounded by a thin and discontinuous ECM (Fig. 4A-i, B-i). No difference in fluorescence intensity was observed between unstimulated (Fig. 4A-iii, B-iii) and PEMF-stimulated cells (Fig. 4A-iv, B-iv) both originating from ASCs.

Regarding the origin of the cell source for the differentiated cells, the immunolocalization of other proteins such as type-I

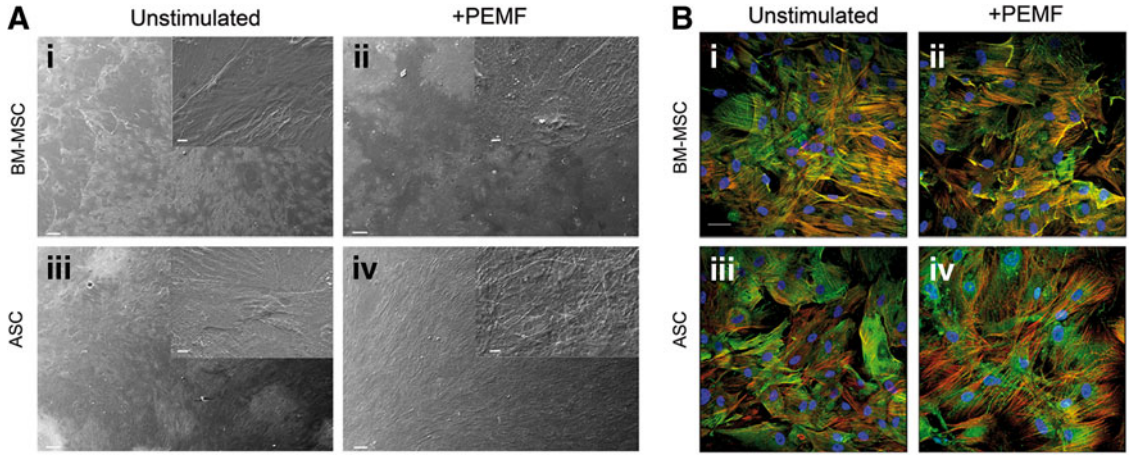

FIG. 2. Effect of PEMF exposure on osteoblast morphology differentiated from BM-MSCs and ASCs after 21 days of incubation, as determined by scanning electron microscopy (SEM) **(A)** and confocal laser scanning microscopy (CLSM) **(B)** analysis. SEM and CLSM observations confirmed equivalent cell morphology in both culture conditions, suggesting that PEMF stimulation did not alter cell viability or proliferation. SEM images **(A)** are at 200× magnification (*insets*, 1000×); scale bars represent 100 μm (*insets*, 10 μm). CLSM images **(B)** are at 40× magnification; scale bar represents 50 μm.

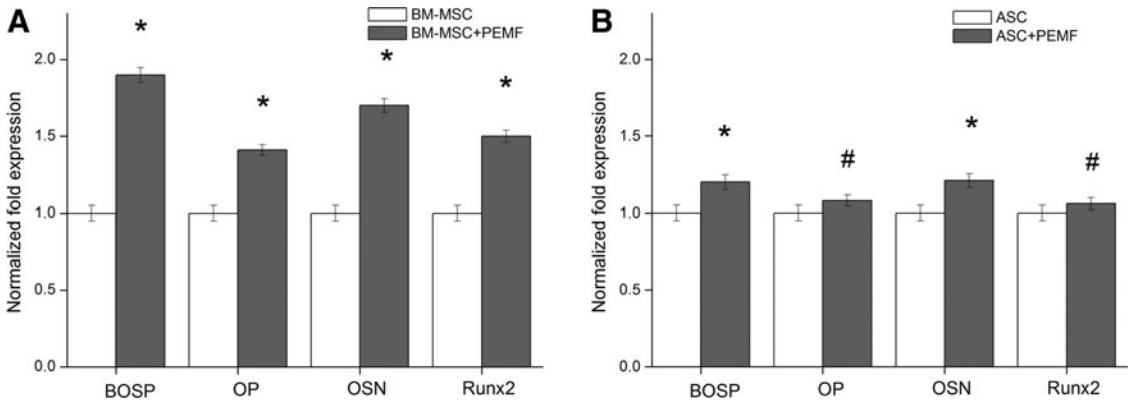

FIG. 3. Effect of PEMF exposure on bone gene expression of the indicated bone-specific markers as determined by quantitative reverse transcriptase–polymerase chain reaction. **(A)** Representative image of osteoblasts differentiated from BM-MSCs. **(B)** Cells differentiated from human adipose tissue. The graph shows the fold induction of gene expression expressed in arbitrary units setting the expressions of the indicated genes in cells grown in absence of PEMF as equal to 1. $*p < 0.001$ was considered statistically significant; $\#p > 0.05$. Data are representative of one of three experiments performed.

collagen, type-III collagen, osteonectin, or FN showed similar patterns (data not shown).

To evaluate the amount of ECM constituents produced by both types of cell in unstimulated or PEMF-stimulated system conditions, an ECM extraction was performed on days 7 and 21. Unfortunately, on day 7 even if the total protein content was determined, the levels of the specific bone proteins were too low to be detected in either sample types. At the end of the culture period, the detection of bone proteins showed some differences. In comparison with the unstimulated culture system, the deposition of bone proteins in the PEMF-treated cells differentiated from BM-MSCs was considerably enhanced ($p < 0.05$) (Table 2). In contrast, this protein deposition was not as marked for osteoblasts differentiated from PEMF-treated ASC compared with unstimulated ASC ($p > 0.05$; Table 2). These data are in accordance with the immunofluorescence analysis performed on unstimulated and PEMF-stimulated culture systems for both cell types (Fig. 4).

Protein deposition was particularly enhanced for ALP, which was 1.7-fold greater compared with unstimulated cells derived from BM-MSCs (Table 2). Again, this difference was not significant between unstimulated and PEMF-stimulated cells differentiated from ASCs. Figure 5 shows the ALP activity measured in both cell types at the end of the culture period: the level of ALP activity was consistently higher in cells differentiated from BM-MSCs and treated with PEMF than in unstimulated cells ($p < 0.001$; Fig. 5B). In contrast, the ALP level was not different in cells of ASC origin, PEMF-stimulated or not (Fig. 5B). These data for cells differentiated from BM-MSCs or ASCs are in accordance with the immunolocalization of ALP in unstimulated (Fig. 5A-i, iii) and PEMF-stimulated culture systems for both cell types (Fig. 5A-ii, iv).

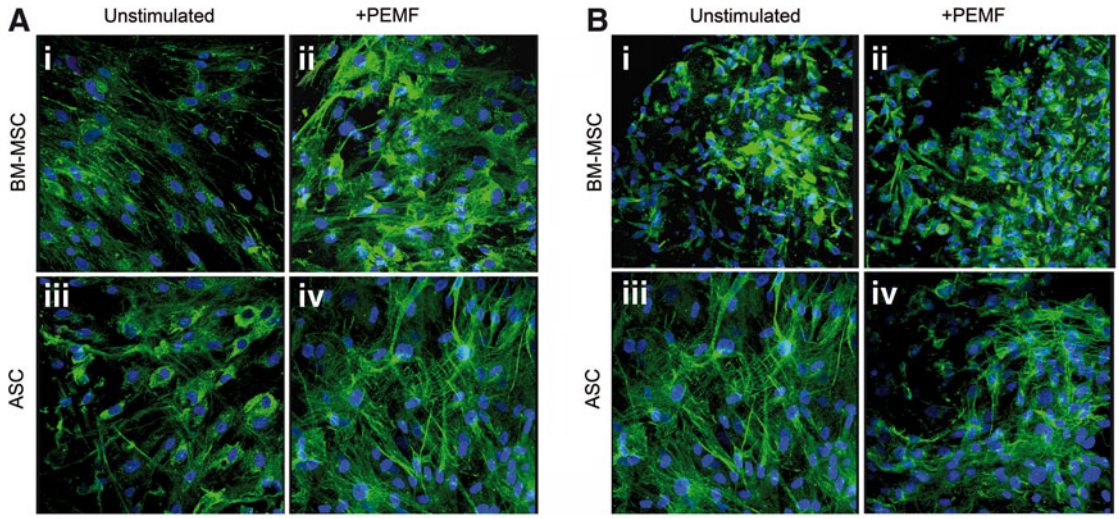

FIG. 4. Effect of PEMF exposure on BM-MSC and ASC osteogenic differentiation as determined by immunolocalization of type-I collagen **(A)** and osteocalcin **(B)** at day 21 of incubation at 40× magnification; scale bar represents 50 μm. The dense layer of bone extracellular matrix was clearly evidenced by an intense fluorescence signal in the PEMF stimulated cells derived from BM-MSCs **(ii)** in comparison with unstimulated BM-MSCs **(i)** or unstimulated ASCs **(iii)**/PEMF stimulated **(iv)** but derived by ASCs.

Table 2. Extracellular Matrix Constituents Secreted and Deposited by Osteoblasts Differentiated from Bone Marrow Mesenchymal Stem Cells and Adipose Tissue Mesenchymal Stem Cells With or Without Pulsed Electromagnetic Field Stimulation After 21 Days of Cell Culture

	Matrix protein deposition after 21 days of cell culture [expressed as pg/(cells per well)]					
Bone proteins	*BM-MSC control*	*BM-MSC + PEMF*	*Ratio BM-MSC + PEMF/BM-MSC*	*ASC control*	*ASC + PEMF*	*Ratio ASC + PEMF/ASC*
Alkaline phosphatase	75 ± 2.2	105 ± 3.5	1.7*	67.33 ± 20	87.52 ± 2.6	1.3
Decorin	70 ± 2.1	84 ± 2.3	1.2	37 ± 1.5	41 ± 2.27	1.1
Fibronectin	38 ± 2.8	46 ± 2.1	1.2	28 ± 1.28	32 ± 2.13	1.14
Osteocalcin	17 ± 1.1	24 ± 1.4	1.4*	15 ± 1.15	17 ± 1.34	1.14
Osteonectin	20 ± 1.3	26 ± 1.2	1.3	16 ± 1.26	21 ± 1.11	1.3
Osteopontin	36 ± 2.3	65 ± 1.4	1.8*	28 ± 1.11	34 ± 3.19	1.2
Type-I collagen	460 ± 6.0	736 ± 6.4	1.6*	200 ± 2.9	230 ± 6.8	1.15
Type-III collagen	90 ± 4.1	126 ± 2.1	1.4*	35 ± 1.2	42 ± 3.2	1.2

*In comparison to unstimulated samples, a p value < 0.05 was considered statistically significant.

The relative amount of calcium for both types of cells and culture system condition was evaluated by the calcein method (Fig. 6A) and quantified by the calcium–cresolphthalein complexone method (Fig. 6B) to evaluate matrix calcification. Figure 6 shows a qualitative assessment of cell and calcium deposition by both cell types in unstimulated and PEMF-stimulated culture conditions with some significant differences: the mineralization of ECM produced by osteoblasts gave a more intense green fluorescence signal colocalized within the cells on PEMF-stimulated than on unstimulated BM-MSCs or PEMF-stimulated cells originating from ASCs. The qualitative evaluation of calcium deposition was confirmed: calcification of the deposited ECM was considerably greater in PEMF-stimulated cells of human BM origin (Fig. 6A-ii) than in unstimulated controls (Fig. 6A-i; $p < 0.05$). In contrast, no difference was observed between unstimulated and PEMF-stimulated cells of human adipose tissue origin (Fig. 6A-iii, iv).

Discussion

Research oriented at isolation of stem cells, their culture for purposes such as developing cell or tissue therapies, differentiation studies, the comprehension of the factors necessary to direct cell specialization to specific pathways, and other developmental studies is an absolute priority in tissue engineering and regenerative medicine, which is an emerging multidisciplinary field involving biology, medicine, engineering, and biomaterials science. Furthermore, the application of an appropriate physical stimulus, such as an electromagnetic field, to mesenchymal stem cells in culture has been reported as a valuable approach to overcome the drawbacks associated with standard culture systems, such as limited diffusion, nonhomogeneous cell-matrix distribution, and reduced cell proliferation and differentiation.[36] To the best of our knowledge the PEMF effects either in stem cells isolated from adipose tissue and/or comparative studies with BM-MSCs have not been investigated. To this end, the main aim of this study was to show the greater efficacy of PEMF exposure on the osteogenic differentiation of BM-MSCs in comparison with ASCs, by evaluating cell proliferation, morphology, and calcified matrix deposition. The increase in differentiation observed for both types of MSCs independent of their tissue origin could be of interest in other clinical settings or in a tissue engineering approach.

In a previous study by our group we showed that cell stimulation using an electromagnetic bioreactor (magnetic field intensity, 2 mT; frequency, 75 Hz) significantly increased SAOS-2 human osteoblast proliferation and bone ECM deposition.[36] In this study, we investigated the effects of electromagnetic stimulation on osteogenesis of stem cells isolated from BM and adipose tissue. When we performed

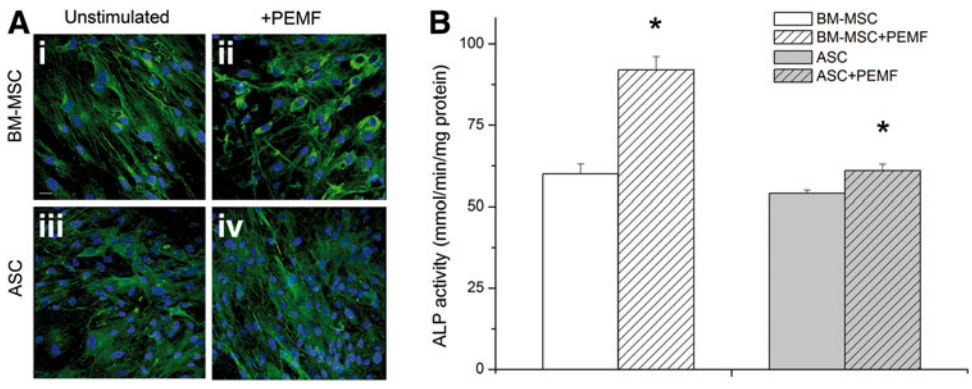

FIG. 5. Effect of PEMF exposure on alkaline phosphatase (ALP) deposition **(A)** and enzyme activity **(B)** by both types of differentiated cell as determined by CLSM (40× magnification; scale bar represents 50 μm) and colorimetrically expressed as millimoles of p-nitrophenol produced per minute per milligram of protein. Bars indicate mean values ± standard error of the mean of results from three experiments (*$p < 0.05$).

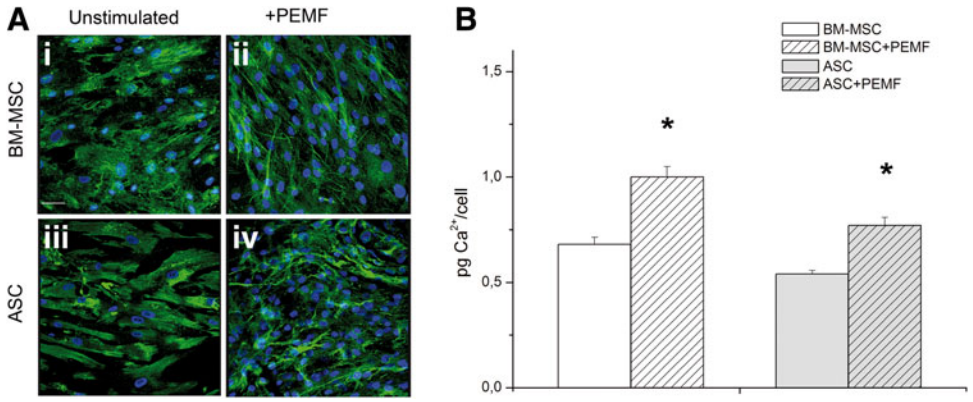

FIG. 6. Effect of PEMF exposure on mineralization of extracellular matrix produced by osteoblasts differentiated from BM-MSCs and ASCs as determined by CLSM **(A)** (40× magnification; scale bar represents 50 μm) and by quantification of calcium content **(B)**. Results are expressed on a per-scaffold basis and are presented as an average ± standard deviation (*$p < 0.05$).

experiments for the same length of time as that utilized for SAOS-2 cell stimulation, the BM-MSCs and ASCs did not survive. In fact, the best results in terms of cell proliferation were achieved by stimulating with the electromagnetic bioreactor both stem cells for 10 min a day with the same physical parameters. Even though, the SAOS-2 cell line is useful to screen different types of culture condition, primary cells (osteoblasts or MSCs) are more relevant and should be used to assess *in vitro* the best physical parameters for electromagnetic stimulation to increase or improve biological mineralization.[36]

A temporal and functional pattern of gene expression characterizes the osteoblast maturation process, which can be divided into proliferation, differentiation, and mineralization stages,[44] in turn the effects of a pulsed electromagnetic field depend on the maturation stages of the osteoblasts.[35,45] PEMF-stimulated osteoblasts of BM origin exhibited a more evident increase in cell proliferation than those of adipose tissue origin. These results are in line with previous data demonstrating that application of PEMF to BM-MSCs cultured in OM results in early onset of cell proliferation and, consequently, higher cell densities.[35] PEMF not only affects osteoblast cellular proliferation and differentiation of bone cells *in vitro* by enhancing DNA synthesis,[34,45,46] but also increases expression of bone marker genes during differentiation and mineralization and enhances calcified matrix production.[34] In order to study the effects of PEMF on ECM deposition for both types of culture condition, the fundamental bone matrix constituents such as type-I and -III collagen, decorin, osteopontin, osteocalcin, osteonectin, and fibronectin were investigated. Both types of PEMF-stimulated cells were able to significantly increase ECM deposition with respect to unstimulated cells. In a comparative quantitative protein analysis between BM-SMCs and ASCs we observed some differences. In both cell types exposed to PEMF, the deposition of type-I and -III collagen and decorin was approximately 1.4-, 1.2-, and 1.1-fold greater, respectively, in wells seeded with BM-MSCs in comparison with ASCs. Bone type-I collagen synthesis is known to be up-regulated at the proliferation stage when the osteoblasts are not confluent, and down-regulated at subsequent stages.[44,47] Both types of protein, type-III collagen and decorin, are known to be associated with type-I collagen.[48] Appreciable differences for other bone matrix proteins such as osteonectin and fibronectin were not detected, with the exception of osteopontin and osteocalcin: 1.5- and 1.2-fold increases in deposition were observed in cultured BM-MSCs and ASCs, respectively. All of these ECM proteins are organic components of bone and are implicated in bone formation and remodeling. Osteopontin is known to play an important role in cell attachment[49] and calcification of mineralized tissue,[50] whereas osteocalcin[51] is the most recently identified secreted ECM protein. Osteonectin is a calcium and collagen-binding ECM glycoprotein and also acts as a modulator of cell–matrix interactions.[52] The role of fibronectin is important considering that it is reported to promote both cell adhesion and proliferation in many cell types.[53,54]

In view of this information, macroscopic increases in *in vitro* protein levels of ALP (makes the phosphate available for calcification), osteopontin (anchors bone cells via their $\alpha_v\beta_3$ integrin to the mineralized bone surface), osteocalcin (a marker of formed bone tissue), and type-I and -III collagens (the major organic components of bone matrix produced by osteoblasts) were more evident for osteoblasts deriving from BM-MSCs than from ASCs (Table 2).

All together these results suggest that the main effect of cell exposure to PEMF is a greater efficiency in promoting bone ECM deposition by osteoblasts differentiating from BM-MSCs.

Interestingly, the qRT-PCR analysis showed an increase in bone sialoprotein, osteopontin, osteonectin, and Runx2 gene expression levels from both types of PEMF-stimulated osteoblasts, at a higher level for BM-MSC differentiated cells in comparison with adipose tissue maturated stem cells. Since osteonectin and osteopontin are critical in mediating the signal cascade for the full expression of the mature osteoblast phenotype and mineralization of the ECM,[55,56] the higher OSN and OP gene expression in both cell types could be related to the cell's ability to better differentiate toward mature osteoblasts and to deposit mineralized bone matrix as a result of PEMF exposure. This concept is also true for BOSP, which is a significant component of the bone ECM and is suggested to constitute approximately 8% of all noncollagenous proteins found in bone and cementum. Furthermore, we decided to evaluate the gene expression level of Runx2, also known as core binding factor 1 (cbfa1; subsequently renamed Runx2 as runt-related transcription factor 2).[57] Runx2 is a transcriptional factor involved in osteoblastic and skeletal morphogenesis. Runx2 has an essential role in the maturation of osteoblasts by binding to its target promoters and enhancers of various other bone-specific target genes, including collagen type-I, osteopontin, and bone sialoprotein through its runt homology domain.[58,59] The Runx2 gene expression in both types of unstimulated cell perfectly correlates with the cell's

ability to differentiate towards osteoblasts. However, Runx2 expression was more enhanced by PEMF exposure in BM-MSCs than ASCs. Since Runx2 is considered the transcriptional target of Wnt/b-catenin pathway,[60] its up-regulation in both types of stem cells during PEMF exposure may due to the activation of the Wnt/b-catenin signaling pathway.[61] However, the electromagnetic application seems to show a stimulatory effect in osteoblasts differentiated from ASCs, but slightly lower when compared with osteoblasts originating from BM-MSCs. Following PEMF exposure, the Wnt/b-catenin signaling pathway is possibly activated in BM-MSCs but other signaling pathways may be stimulated in ASCs. Recently, it was shown that the exposure of ASCs cells to a 45-Hz electromagnetic field induced osteogenic marker expression via bone morphogenetic protein, transforming growth factor β, and Wnt signaling pathways based on microarray analyses.[62]

In summary, the increased transcription of these genes could indicate that PEMF exposure drives a more rapid commitment of stem cells toward osteoblastic differentiation, in particular for BM-MSCs, but to a lower extent for ASCs.

The increase in transcript levels of the BOSP, OSN, and OP genes was supported by the mineralization data. Quantitative analysis of the calcium mineral content showed that both types of PEMF-stimulated cells were able to deposit a significantly higher amount of newly mineralized matrix compared with unstimulated cells. In a quantitative comparative analysis, an approximate 1.5-fold difference in matrix calcification was detected for BM-MSC–derived osteoblasts with respect to ASCs. Furthermore, confocal microscopic analysis evidenced calcification and bone matrix proteins in the cell-rich area for both types of cells, with a stronger fluorescence signal for cells differentiated from BM.

In this study, the increase in calcium deposition was consistent with the rise in ALP expression in both types of PEMF-exposed MSCs. In a comparison analysis with ASC-derived osteoblasts, the protein content was 1.3-fold greater for cells differentiated from BM-MSCs. ALP activity also increase by almost 2-fold. ALP is recognized as an important component in hard tissue formation and is highly expressed in mineralized tissue cells. Osteoblast cells grown with ascorbic acid sequentially express osteoblastic marker proteins such as ALP and then form a mineralized ECM as a consequence of osteoblastic differentiation. The importance of ALP in the mineralization of ECM has been previously reported.[63] Its mechanism of action is not completely known, but it appears to promote both the local concentration of inorganic phosphate, a mineralization promoter, and to decrease the concentration of extracellular pyrophosphate, an inhibitor of mineral formation.[63] Previous studies have reported that ALP is expressed in large amounts in osteoblasts *in vivo*.[64] The elevated expression of ALP (which occurs at the end of the cell proliferative state), osteopontin and bone sialoprotein may suggest that the MSC-derived osteoblasts are more differentiated than ASC osteoblasts and have already started to promote bone ECM deposition.

Although ASCs and BM-MSCs share many biological characteristics, there are some differences in their immunophenotype, differentiation potential, transcriptome, proteome, and immunomodulatory activity.[65] A possible explanation of why BM-MSCs showed a more rapid osteogenic differentiation than ASCs when treated with PEMF could be related to their differences such as specific features of BM-MSCs and ASCs, or it could be due to the inherent heterogeneity of both BM-MSC and ASC populations or to a different activation of a signaling pathway.

In summary, these results suggest that PEMF enhances the commitment of BM-MSCs to osteoblasts more efficiently in comparison with ASCs. Both types of mesenchymal stem cells are osteogenic (Table 2), but in an tissue engineering approach, which combines biomaterials, growth factors, and cells, the ASC exposure to PEMF seem to be less effective. Furthermore, PEMF *in vitro* studies should be considered as groundwork for *in vivo* bone development that may support skeletal therapy. Taken all together, these findings may provide insights on the development of PEMF as an effective technology for regenerative medicine.

Acknowledgments

This work was supported by the Compagnia S. Paolo (Genova) Grant titled "Uso di cellule staminali mesenchimali sottoposte a campo elettromagnetico: un approccio innovativo per l'osteointegrazione di impianti di titanio" (2011) to L.V. and by an INAIL grant entitled "Effetti dei campi elettromagnetici sulla salute umana: modelli sperimentali in vitro" (2011) to G.C. We are grateful to P. Vaghi (Centro Grandi Strumenti, University of Pavia) and D. Picenoni (Politecnico di Milano, Milano, Italy) for technical assistance in the CLSM and SEM studies, respectively. A special thanks to Laurene Kelly (University of Pavia) for correcting the English in the manuscript.

Author Disclosure Statement

All the authors state that no competing financial interests exist.

References

1. Bunnell BA, Flaat M, Gagliardi C, et al. Adipose-derived stem cells: Isolation, expansion and differentiation. Methods. 2008;45:115–120.
2. Kuroda Y, Kitada M, Wakao S, et al. Bone marrow mesenchymal cells: how do they contribute to tissue repair and are they really stem cells? Arch Immunol Ther Exp. 2011;59:369–378.
3. Shekkeris AS, Jaiswal PK, Khan WS. Clinical applications of mesenchymal stem cells in the treatment of fracture non-union and bone defects. Curr Stem Cell Res Ther. 2012;7:127–133.
4. Kon E, Filardo G, Roffi A, et al. Bone regeneration with mesenchymal stem cells. Clin Cases Miner Bone Metab. 2012; 9:24–27.
5. Izadpanah R, Trygg C, Kriedt BPC, et al. Biologic properties of mesenchymal stem cells derived from bone marrow and adipose tissue. J Cell Biochem. 2006; 99:1285–1297.
6. Witkowska-Zimny M, Walenko Z. Stem cells from adipose tissue. Cell Mol Biol Lett. 2011;16:236–257.
7. Tapp H, Hanle N, Patt J, et al. Adipose-derived stem cells: characterization and current application in orthopaedic tissue repair. Exp Biol Med. 2009;234:1–9.
8. Strem BM, Hicok KC, Zhu M, et al. Multipotential differentiation of adipose tissue-derived stem cells. Keio J Med. 2005; 54:132–141.
9. Bruder SP, Jaiswal N, Haynesworth SE. Growth kinetics, self-renewal, and the osteogenic potential of purified human mesenchymal stem cells during extensive subcultivation and following cryopreservation. J Cell Biochem. 1997;64: 278–294.

10. De Ugarte DA, Morizono K, Elbarbary A, et al. Comparison of multi-lineage cells from human adipose tissue and bone marrow. Cell Tissues Organs. 2003;174:101–109.
11. Saino E, Fassina L, Van Vlierberghe S, et al. Effects of electromagnetic stimulation on osteogenic differentiation of human mesenchymal stromal cells seeded onto gelatin cryogel. Int J Immunopathol Pharmacol. 2011;24(1 Suppl. 2):1–6.
12. Hu Y, Cai K, Luo Z, et al. Regulation of the differentiation of mesenchymal stem cells in vitro and osteogenesis *in vivo* by microenvironmental modification of titanium alloy surfaces. Biomaterials. 2012;33:3515–3528.
13. Hoshiba T, Kawazoe N, Chen G. The balance of osteogenic and adipogenic differentiation in human mesenchymal stem cells by matrices that mimic stepwise tissue development. Biomaterials. 2012;33:2025–2031.
14. Kavlock KD, Goldstein AS. Effect of pulse frequency on the osteogenic differentiation of mesenchymal stem cells in a pulsatile perfusion bioreactor. J Biomech Eng. 2011;133:091005.
15. Kim J, Ma T. Perfusion regulation of hMSC microenvironment and osteogenic differentiation in 3D scaffold. Biotechnol Bioeng. 2012;109:252–261.
16. Carpentier B, Layrolle P, Legallais C. Bioreactors for bone tissue engineering. Int J Artif Organs. 2011;34:259–270.
17. Massari L, Caruso G, Sollazzo V, et al. Pulsed electromagnetic fields and low intensity pulsed ultrasound in bone tissue. Clin Cases Miner Bone Metab. 2009;6:149–154.
18. Midura RJ, Ibiwoye MO, Powell KA, et al. A. Pulsed electromagnetic field treatments enhance the healing of fibular osteotomies. J Orthop Res. 2005;23:1035–1046.
19. Walker NA, Denegar CR, Preische J. Low-intensity pulsed ultrasound and pulsed electromagnetic field in the treatment of tibial fractures: a systematic review. J Athl Train. 2007;42: 530–535.
20. Ciombor DM, Aaron RK. Influence of electromagnetic fields on endochondral bone formation. J Cell Biochem. 1993;52: 37–41.
21. Otter MW, McLeod KJ, Rubin CT. Effects of electromagnetic fields in experimental fracture repair. Clin Orthop Relat Res. 1998;355(Suppl):S90–S104.
22. Huang LQ, He HC, He CQ, et al. Clinical update of pulsed electromagnetic fields on osteoporosis. Chin Med J (Engl). 2008;121:2095–2099.
23. Midura RJ, Ibiwoye MO, Powell KA, et al. Pulsed electromagnetic field treatments enhance the healing of fibular osteotomies. J Orthop Res. 2005;23:1035–1046.
24. Heckman JD, Ingram AJ, Loyd RD, et al. Nonunion treatment with pulsed electromagnetic fields. Clin Orthop Relat Res. 1981;161:58–66.
25. Friedenberg ZB, Brighton CT. Bioelectric potentials in bone. J Bone Joint Surg Am. 1966;48:915–923.
26. de Haas WG, Watson J, Morrison DM. Non-invasive treatment of ununited fractures of the tibia using electrical stimulation. J Bone Joint Surg Br. 1980;62B:465–70.
27. Grace KL, Revell WJ, Brookes M. The effects of pulsed electromagnetism on fresh fracture healing: osteochondral repair in the rat femoral groove. Orthopedics. 1998;21:297–302.
28. Korbling M, Estrov Z. Adult stem cells for tissue repair—a new therapeutic concept? N Engl J Med. 2003;349:570–582.
29. Beresford JN. Osteogenic stem cells and the stromal system of bone and marrow. Clin Orthop Relat Res. 1989;240: 270–280.
30. Pittenger MF, Mackay AM, Beck SC, et al. Multilineage potential of adult human mesenchymal stem cells. Science. 1999;284:143–147.
31. Halleux C, Sottile V, Gasser JA, et al. Multi-lineage potential of human mesenchymal stem cells following clonal expansion. J Musculoskelet Neuronal Interact. 2001;2: 71–76.
32. Fitzsimmons RJ, Ryaby JT, Magee FP, et al. Combined magnetic fields increased net calcium flux in bone cells. Calcif Tissue Int. 1994;55:376–380.
33. Pavalko FM, Norvell SM, Burr DB, et al. A model for mechanotransduction in bone cells: The load-bearing mechanosomes. J Cell Biochem. 2003;88:104–112.
34. Tsai MT, Chang WH, Chang K, et al. Pulsed electromagnetic fields affect osteoblast proliferation and differentiation in bone tissue engineering. Bioelectromagnetics. 2007;28: 519–528.
35. Sun LY, Hsieh DK, Lin PC, et al. Pulsed electromagnetic fields accelerate proliferation and osteogenic gene expression in human bone marrow mesenchymal stem cells during osteogenic differentiation. Bioelectromagnetics. 2010;31: 209–219.
36. Fassina L, Saino E, Visai L, et al. Electromagnetic enhancement of a culture of human SAOS-2 osteoblasts seeded onto titanium fiber-mesh scaffolds. J Biomed Mater Res A. 2008;87:750–759.
37. Bernardo ME, Zaffaroni N, Novara F, et al. Human bone marrow derived mesenchymal stem cells do not undergo transformation after long-term in vitro culture and do not exhibit telomere maintenance mechanisms. Cancer Res. 2007; 67:9142–9160.
38. Romanov YA, Darevskaya AN, Merzlikina NV, et al. Mesenchymal stem cells from human bone marrow and adipose tissue: isolation, characterization, and differentiation potentialities. Cell Technol Biol Med. 2005;3:138–143.
39. Bernardo ME, Avanzini MA, Perotti C, et al. Optimization of in vitro expansion of human multipotent mesenchymal stromal cells for cell-therapy approaches: further insights in the search for a fetal calf serum substitute. J Cell Physiol. 2007; 211:121–130.
40. Saino E, Grandi S, Quartarone E, et al. In vitro calcified matrix deposition by human osteoblasts onto a zinc-containing bioactive glass. Eur Cell Mater. 2011;21:59–72.
41. van Engeland M, Nieland LJW, Ramaekers FCS, et al. Annexin v-affinity assay: a review on an apoptosis detection system based on phosphatidylserine exposure. Cytometry. 1998;31:1–19.
42. Saino E, Maliardi V, Quartarone E, et al. In vitro enhancement of SAOS-2 cell calcified matrix deposition onto radio frequency magnetron sputtered bioglass-coated titanium scaffolds. Tissue Eng Part A. 2010;16:995–1008.
43. Cohen SA, Sideman L. Modification of the o-cresolphthalein complexone method for determining calcium. Clin Chem. 1979;25:1519–1520.
44. Owen TA, Aronow M, Shalhoub V, et al. Progressive development of the rat osteoblast phenotype in vitro: reciprocal relationships in expression of genes associated with osteoblast proliferation and differentiation during formation of the bone extracellular matrix. J Cell Physiol. 1990;143:420–430.
45. Diniz P, Shomura K, Soejima K, et al. Effects of pulsed electromagnetic field (PEMF) stimulation on bone tissue like formation are dependent on the maturation stages of the osteoblasts. Bioelectromagnetics. 2002;23:398–405.
46. De Mattei M, Caruso A, Traina GC, et al. Correlation between pulsed electromagnetic fields exposure time and cell proliferation increase in human osteosarcoma cell lines and

human normal osteoblast cells in vitro. Bioelectromagnetics. 1990;20:177–182.
47. Selvamurugan N, Kwok S, Vasilov A, et al. Effects of BMP-2 and pulsed electromagnetic field (PEMF) on rat primary osteoblastic cell proliferation and gene expression. J Orthop Res. 2007;25:1213–1220.
48. Quarles LD, Yohay DA, Lever LW, et al.. Distinct proliferative and differentiated stages of murine MC3T3-E1 cells in culture: an in vitro model of osteoblast development. J Bone Miner Res. 1992;**7:**683–692.
49. Azari F, Valli H, Guerquin-Kern J, et al. Intracellular precipitation of hydroxyaptite mineral and implications for pathological calcification. J Struct Biol. 2008;162:468–479.
50. Van Dijk S, D' Errico JA, Somemen MJ, et al. Evidence that a non-RGD domain in rat osteopontin is involved in cell attachment. J Bone Miner Res. 1993;8:1499–1506.
51. Denhardt DT, Guo X. Osteopontin: a protein with diverse functions. FASEB J. 1993;**7:**1475–1482.
52. Aubin JE, Liu F. The osteoblast lineage. In: *Principles of Bone Biology*. Bilezkian JP, Raisz LG, Rodan GA (eds). Academic Press: San Diego, CA; pp. 51; 1996.
53. Grzesik WJ, Robey PG. Bone matrix RGD glycoproteins: immunolocalization and interaction with human primary osteoblastic bone cells in vitro. J Bone Miner Res. 1994;9: 487–496.
54. Krämer A, Horner S, Willer A, et al. Adhesion to fibronectin stimulates proliferation of wild-type and bcr/abl transfected murine hematopoietic cells. Proc Natl Acad Sci USA. 1999;96: 2087–2092.
55. Wilson SH, Ljubimov AV, Morla AO, et al. Fibronectin fragments promote human retinal endothelial cell adhesion and proliferation and ERK activation through alpha5beta1 integrin and PI 3-kinase. Invest Ophthalmol Vis Sci. 2003;44: 1704–1715.
56. Lynch MP, Stein JL, Stein GS, et al. The influence of type I collagen on the development and maintenance of the osteoblast phenotype in primary and passaged rat calvarial osteoblasts: modification of expression of genes supporting cell growth, adhesion, and extracellular matrix mineralization. Exp Cell Res. 1995;216:35–45.
57. Kojima H, Uede T, Uemura T. In vitro and in vivo effects of the overexpression of osteopontin on osteoblast differentiation using a recombinant adenoviral vector. J Biochem. 2004; 136:377–386.
58. Komori T. Regulation of osteoblast differentiation by transcription factors. J Cell Biochem. 2006;99:1233–1239.
59. Otto F, Lübbert M, Stoc M. Upstream and downstream targets of RUNX proteins. J Cell Biochem. 2003;89:9–18.
60. Gaur T, Lengner CJ, Hovhannisyan H, et al. Canonical WNT signaling promotes osteogenesis by directly stimulating Runx2 gene expression. J Biol Chem. 2005;280:33132–33140.
61. Zhou J, He H, Yang L, et al. Effects of pulsed electromagnetic fields on bone mass and Wnt/b-catenin signaling pathway in ovariectomized rats. Arch Med Res. 2012;43:274–282.
62. Kang KS, Hong JM, Seol YJ, et al. Short-term evaluation of electromagnetic field pretreatment of adipose-derived stem cells to improve bone healing. J Tissue Eng Regen Med. 2012 Dec 26 [Epub ahead of print]; DOI: 10.1002/term.1664.
63. Torii Y, Hitomifl K, Yamagishi, Y, et al. Demonstration of alkaline phosphatase participation in the mineralization of osteoblasts by antisense RNA approach. Cell Biol Int. 1996; 20:459–464.
64. Zernick J, Twarog K, Upholt WB. Regulation of alkaline phosphatase and alpha 2(1) procollagen synthesis during early intramembranous bone formation in the rat mandible. Differentiation. 1990;44:207–215.
65. Strioga M, Viswanathan S, Darinskas A, et al. Same or not the same? Comparison of adipose tissue-derived versus bone marrow-derived mesenchymal stem and stromal cells. Stem Cells Dev. 2012;21:2724–2752.

Address correspondence to:
Livia Visai, PhD
Department of Molecular Medicine
University of Pavia
Viale Taramelli 3/B
27100 Pavia
Italy

E-mail: lvisai@unipv.it